Influence of Deflection Deformations on the Sustainability of the Landfill Cover: Analysis and Recommendations

Mehrez Jamei
Civil Engineering Department, College of Engineering, Northern Border University, Saudi Arabia
mehjamei@yahoo.fr

Abdelkader Mabrouk
Civil Engineering Department, College of Engineering, Northern Border University, Saudi Arabia
abdjih2019@gmail.com (corresponding author)

Yahya Alassaf
Civil Engineering Department, College of Engineering, Northern Border University, Saudi Arabia
alassafy@gmail.com

Received: 27 March 2024 | Revised: 10 April 2024 | Accepted: 12 April 2024

 DOI: https://doi.org/10.48084/etasr.7364

ABSTRACT

The design of cover landfill requires an optimum thickness of the compacted fine soil layer with small permeability. In general, the objective is to reduce the thickness of the landfill cover. However, for a thin layer, and under natural evaporation, denser crack network growths occur during the desiccation by drying. Cracks change the geometrical properties during the drying and wetting cycles and significantly compromise the role of the cover layer, by inducing an infiltration water flow and gas migration. An important differential flexure deformation occurs. The landfill cover, where stiffness and tensile and shear strengths were reduced is being progressively damaged. Thus, this paper aims 1) to quantify the flexural deformation and 2) to provide a methodology and a guideline for studying the integrity of a cover landfill. So, a mechanical model is proposed and implemented in Code Bright software. The methodology starts from the calibration and the validation of the mechanical model based on 1) four-point flexural beam tests and 2) on existing published results. A physical prototype was employed to demonstrate the flexure deformation, and the crack development. Moreover, short natural fibers were mixed and embedded in the soil to make the soil reinforcement and delay crack propagation. In addition to the experimental investigation, mathematical constitutive equations were proposed, in which the contribution of short fibers in terms of increase of tensile strength was introduced. Finally, a simple case study was considered to demonstrate the role of the fiber-soil composite on flexural deformation and tensile stress distribution across the cover layer. An analysis of the numerical results was conducted to support the use of short fibers as reinforcement, which is an environmentally friendly and sustainable solution.

Keywords-cover landfill; desiccation cracks; deformationn; beam tests; flexure modeling; fibers; reinforcement

I. INTRODUCTION

The controlled landfill surface storage of non-radioactive solid waste has been developed to preserve the environment by developing a convenient waste management policy [1-3]. As an example, according to the Saudi Arabia National Center for Waste Management, the environmental degradation caused by solid waste in 2021 was estimated at $1.3 billion. Also, according to the former CEO of the Saudi Investment Recycling Company, most of the country's waste is currently being landfilled at an average of $1.87 per ton and the incineration technique is increasingly being neglected and abandoned [4]. Landfill space has been managed according to a main rule, which is based on the protection of the soil against the infiltration, lixiviation, and gas produced by the biologic process of solid waste transformation during long landfill deposition [5-7]. Landfill cover is designed to prevent the infiltration of water, the release of gases, and the migration of contaminants from the waste material into the surrounding environment. The deflection of the cover can be influenced by various factors, including the design and construction of the cover system, the nature and composition of the waste material, and environmental conditions such as temperature and water moisture. Engineering standards and guideline regulations such

as the US Environmental Protection Agency's Subtitle of the Resource Conservation and Recovery Act (RCRA) provide standards for landfill design, construction, operation, and closure. These guidelines often include requirements for landfill cover systems and may address aspects related to cover deflection [8].

Obviously, the control of the bottom of the landfill by a complex associated geomembrane-geotextile composite is now considered as a successful technical solution. From an engineering point of view, its design and application are relatively understandable tasks. However, the issue of the sealing task from the landfill cover is still big and complex. The completely non-homogenous deformation of the cover layers due to the non-homogenous settlement of the solid waste and its heterogeneous physical properties such as water content and dry density is a complex geotechnical problem. In addition, due to variations in the temperature, desiccation cracks can occur, which in turn strongly affect the hydraulic and mechanical properties. In fact, cracks increase the permeability and reduce the mechanical strength. To analyze and predict the flow and transport behavior in cracked unsaturated soils, recently published papers in the geotechnical field have been interested in the unsaturated permeability function [9-11]. Obviously, crack birth and growth are functions of the deflection increment and the development of tensile stress in the zone of landfill cover [12-14]. Monitoring the deflection of the cover is therefore crucial for ensuring its long-term performance and the protection of the environment and public health [15-17]. Techniques, such as slope inclinometers, settlement plates, and surveying methods can be used to measure and track the deflection of the cover over time. By closely monitoring and managing deflection, engineers and landfill operators can identify potential problems early on and implement corrective measures to maintain the integrity and functionality of the landfill cover system [6, 8, 15].

The current paper aims to analyze the deflection of the cover layer, starting from the modeling and the experiments performed on beams of clay built by compaction. Evidently, initial water content and dry density were considered in the modeling because they have a significant influence on the deflection of the beams. A physical prototype has been built to reproduce the deformation and study reinforcement techniques to reduce the deflection. It has been demonstrated that the use of geotextile, which was located at the bottom of the cover layer, significantly reduces deflection. However, despite the local soil-geotextile reinforcement, cracks appear in the soil mass of the cover layer. Thus, the reinforcement of the soil-volume by short fibers, if mixed randomly, reduces crack birth and crack network development. The utilization of silty soil, intended for use for landfill cover due its lesser permeability [8, 18], and modeling based on finite element method with the Code-Bright software [19] are considered. The results are analyzed in terms of vertical displacement and tensile stress. The efficiency of each reinforcement technique is evaluated versus its capability to decrease the vertical displacement of the landfill cover and the crack network propagation [15-17].

II. EXPERIMENTAL STUDY

A. Physical and Mechanical Properties of the Materials

The Grain Size Distribution (GSD) of the soil was determined. To check that the soil structure had not been altered after reconstitution, the Grain Size Curves (GSCs) of the soil before and after reconstitution were also determined. The GSD of non-reconstituted samples was obtained by using the wet sieve analysis method and the hydrometer test. However, the laser technique was adopted for the reconstituted soil. Figure 1 presents the GSDs of soils. It is noticed that the two GSCs are close. The soil is constituted of 60% silt, 5% clay, and 35% fine sand. Table I provides the physical and mineralogical characteristics of the soil. According to ASTM classification, the soil is silt with high plasticity. In this paper, the definition of sandy silt soil is utilized to take into account the percentage of fine sand (35%).

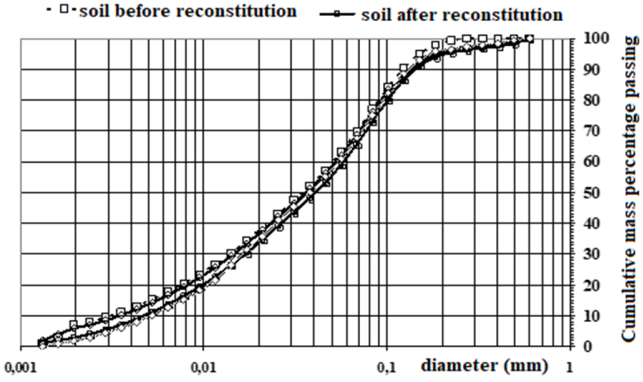

Fig. 1. Grain size distribution of the soil and used fibers.

TABLE I. SOIL CHARACTERISTICS

Sample designation	**Sandy silt soil**
Specific gravity	2.72
Liquid limit-LL (%)	51
Plasticity Index-PI (%)	26
Initial water content, w_i (%)	18
Optimum Water Content-OMC (%)	15
Dry unit density (gr/cm^3)	1.78
Specific surface SST (m^2/gr)	124
Mechanical properties and dimensions of alpha fibers (natural treated fibers)	
Tensile strength (MPa)	54
Elastic tensile modulus (GPa)	18
Average diameter (mm)	0.3
Average length (cm)	3-4

B. Mechanical Properties of the Soil

Compressive and flexure tests have been performed on several samples. Compressive tests were conducted on samples with cylindrical and cubic forms. In fact, cylindrical specimens were prepared (diameter = 10.16 cm, height = 20.32 cm) along with cubic samples from the beam after finishing the bending tests. Figure 3 illustrates images of the two sample types and the corresponding compressive failure modes. Figure 4 portrays the compressive stress curve for the two types of specimens. On the other hand, to characterize the sandy silt to

use in landfill cover, four-point bending tests attempting to reproduce conditions of implementation were carried out in the laboratory. Dimensions of the beam have been optimized to respect the standard definition of the beam dimensions, which should be also convenient for compaction (initial dry density reached by compaction in a prepared mold). The dimensions are 10 cm × 40 cm. Figure 5 displays the flexure test protocol, where the tensile failure mode by flexion is presented and exhibits a typical mode of tensile failure. Three bending tests have been performed by less variation of the initial water content. Obviously, the tensile modulus and the failure force are deduced from the curves obtained for specimens compacted at OMC and tested.

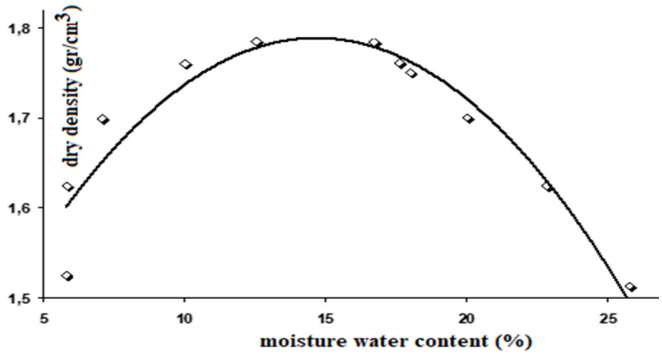

Fig. 2. Proctor compaction curve of the sandy silt.

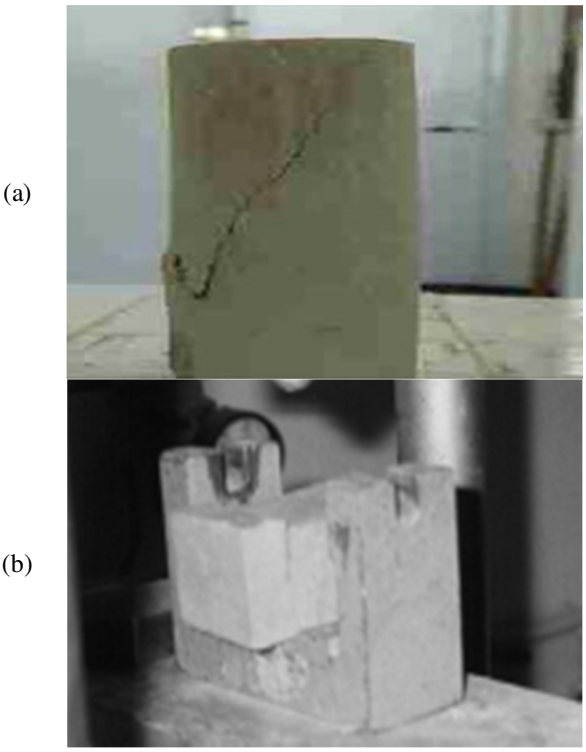

Fig. 3. (a) Failed cylindrical specimen at the end of the compression test, (b) Cubic specimen at the end of the compression test.

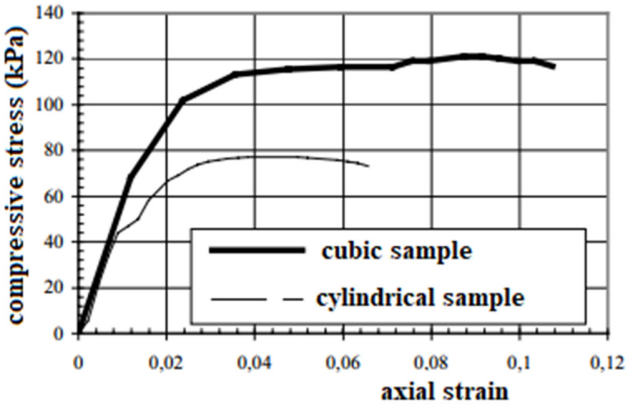

Fig. 4. Compressive stress versus axial strain.

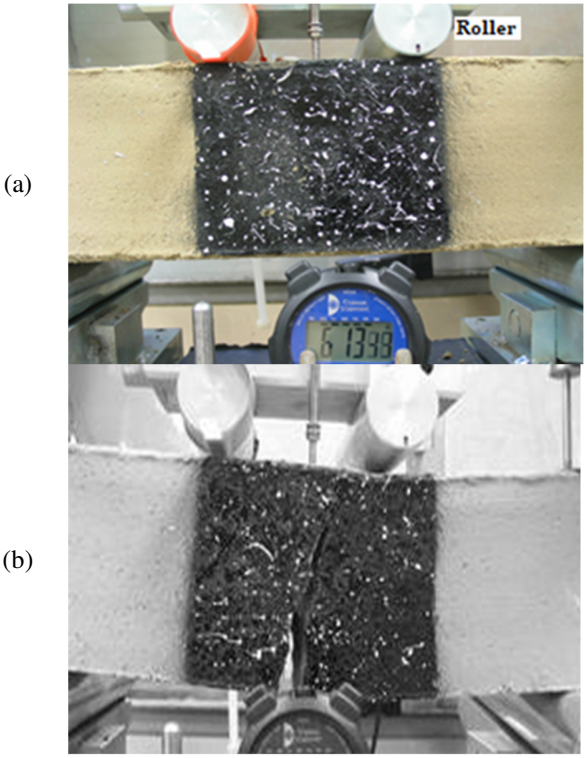

Fig. 5. (a) Bending test on a compacted specimen, (b) tensile failure mode in bending test.

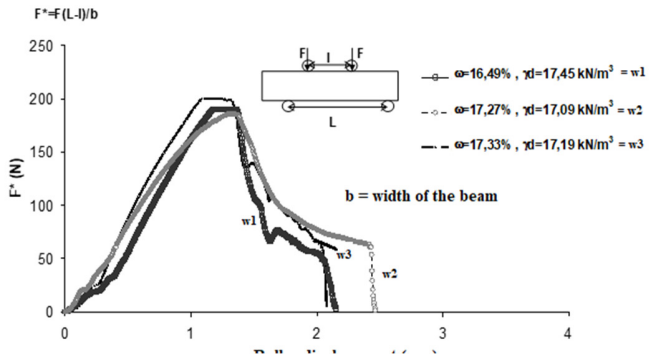

Fig. 6. Bending results of flexure force versus the roller vertical displacement.

The tensile modulus is acquired from the deflection test according to (1):

$$E_t = \frac{1}{d_{max}} \frac{F_{max}\ l^3}{16\ b^4} \quad (1)$$

where d_{max} is the maximum deflection, l is the length between the two top rollers, b is the width of the beam and F_{max} is the maximum force obtained from bending tests (Figure 6).

The tensile and compressive modulus will be used as the main modeling data.

III. MODELING OF FLEXURE TESTS AND APPLICATION TO LANDFILL COVER STABILITY

A. Validation of the Proposed modeling based on Flexure Beam Tests

In this section, the finite element method is adopted utilizing the Code-Bright software [19]. Initially, the model validation takes place using some results from [20]. The results from Code-Bright are observed in Figure 4 in [20]. The former are based on the flexural four-point bending tests on clay with the mechanical properties described in [20] and compared with the data from [20]. The laboratory tests were performed on different specimens of compacted clay with four different initial water content (W) values and with different equivalent Proctor energy rates, $e_c = E_d/E_{dst}$ (where E_{dst} is the standard Proctor energy equivalent to the effort = 450 kN/m^2) [20]. Plane strain elastoplastic finite element analysis was considered. The Mohr–Coulomb failure criterion was chosen to model the soil behavior. The elastoplastic Mohr–Coulomb model involves four input parameters: Young's modulus E, Poisson's ratio v, cohesion, and friction angle φ [20, 21]. There is a a good agreement between the results. Tensile stress damage and shearing bands are often observed in the tested beam in the laboratory. Figure 4 in [20] gives the strain ε_{axx} (%) versus deflection in mm, (where ε_{axx} is here defined as the average deformation according to the x axis on the bottom "line" of the beam, submitted to tensile stress). Figure 7 manifests the mesh of the finite elements engageed in the modeling and the position of the tensile fiber for which the average tensile strain was calculated.

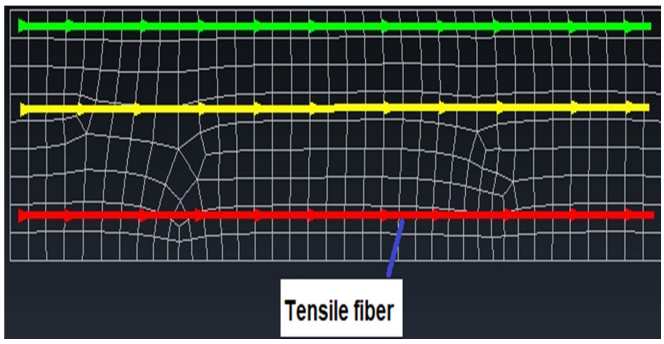

Fig. 7. Deformed finite element mesh in bending test and definition of tensile fiber.

It is useful to indicate that authors in [20, 21] employed image correlation and determined a maximum tensile strain corresponding to crack initiation. Obviously, the model proposed in this paper could not predict the crack birth and its development. So, the average strain is utilized instead of the maximum strain ε_{myy} at crack initiation [20]. The second validation is to reproduce some results of the four-point bending tests carried out in this research and presented in Figure 6. Figure 8 demonstrates the obtained results and reveals a good agreement between modeling and experimental data. However, it is important to mention that in the laboratory, experimental bending tests were performed by controlling the force rate, contrary to the modeling where the displacement rate was controlled.

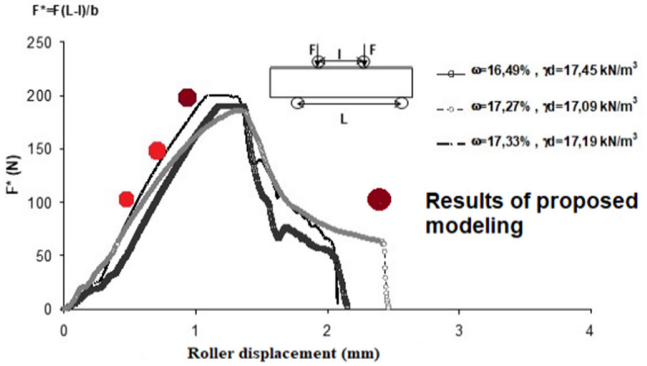

Fig. 8. Validation of the proposed model using four-bending tests (described in Figure 6).

Based on the two types of validation of the numerical modeling, the second step was to model the deflection of a cover landfill with silty sand. The goal is to use numerical simulations to study the role of the volume-reinforcement of the cover landfill deploying short fibers.

B. Modeling based on Flexure Beam Tests

Aiming to study the deflection of a landfill cover and to present a deep analysis of the expected deformation, a reference is primarily made to the following laboratory tests [22] on a reduced physical prototype, showcasing the deflection of part of the soil despite the use of geotextile to reinforce the physical-beam model. To simulate the deformation of the waste mass, clay beads were disposed on the bottom, and then void (cavities) was induced by removing a part of clay beads. Figure 9 displays a photo of the bending-physical prototype. It also demonstrates that the bottom layer works independently as a 0.3 m layer subject to bending under its own weight. Besides the fact that geotextile significantly reduces the deflection (the maximum deflection was of 10 mm), the important finding concerns the development of crack network by tensile in a weak zone of the sub-layer. Obviously, the characteristics of the geotextile can be optimized to currently assure the function needed to reduce the deflection [22].

C. Modeling of the Cover Layer Deflection and Stresses

1) Definition of the Proposed Model

Regarding the limited efficiency of the geotextile to reinforce the upper layer observed across the physical

prototype results, the reinforcement technique has been selected through an introduction of the short fibers embedded randomly in the cover landfill. In fact, it is well known that short fibers embedded in the soil delay crack initiation and increase tensile resistance [23-25]. In this study it is proposed for the influence of fibers to be exclusively modeled on cohesion and consequently on tensile strength as follows:

$$R_t = R_{t0} + \Delta\sigma_{tf}(\theta_f) \quad (2)$$

where R_{t0} is the tensile strength of the soil defined above and reported in Figures 6 and 8, $\Delta\sigma_{tf}$ is the increment of the tensile strength due to reinforcement by fibers, and θ_f is the mass percentage of fibers (mass fibers content). Some researches have been interested to investigate the measurement and then the calculation of the increment (as non-exhaustive publications [13, 26, 27].

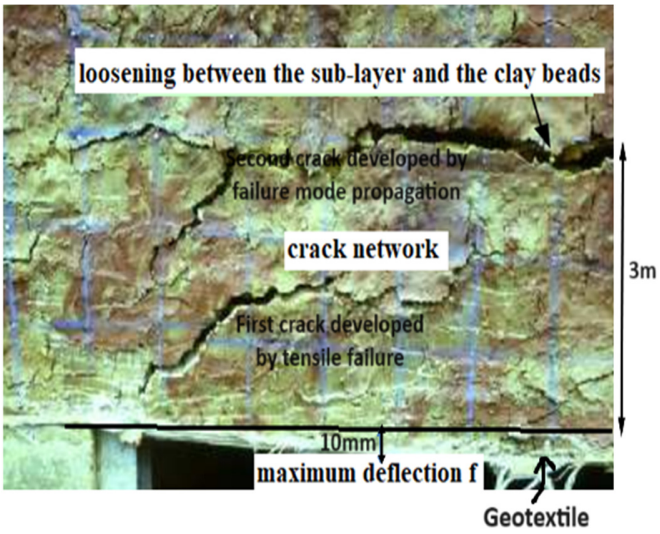

Fig. 9. Deflection of geotextile, the sub-layer and cracks by tensile failure.

The tensile strength is defined here as:

$$R_t = C(\theta_f)\,\text{cotang}(\varphi) \quad (3)$$

where φ is the friction angle assumed independent of the fiber content and $C(\theta_f)$ is the apparent cohesion which depends on θ_f.

Then the apparent cohesion of reinforced soil is obtained as:

$$C(\theta_f) = R_t\, tang(\varphi) \quad (4)$$

The definition given in [23] is assumed, where:

$$\Delta\sigma_{tf}(\theta_f) = \frac{\pi\, d \sum_{i=1}^{i=Nf}(\tau_{fi}\ \zeta_i)}{s} \quad (5)$$

where d is the average diameter of the fibers of 0.3 mm, ζ_i is the active length of each fiber (part of fiber submitted to interfacial shear). It was admitted that the active part of fiber submitted to shear action is $l_i/2$, and l_i is defined by the average value l of 30 mm [23], τ_{fi} is the individual interfacial shear between fibers and soil matrix and s is the tension failure plane area (cross section of tensile failure), assumed as constant for all fibers and equals to the average cross section of the fibers.

$$\theta_f = \frac{M_f(1+w)}{M_m} \quad (6)$$

Considering the assumptions, (4) becomes:

$$\Delta\sigma_{tf}(\theta_f) = \frac{\pi\, d\ N_f\ \tau_f\ l}{s} = 4\ \frac{l}{d}\ N_f\ \tau_f \quad (7)$$

As was demonstrated in [26], the expected number of fiber per unit volume is:

$$N_v = \frac{4\ c_f}{\pi\, D_f^2\ l\ (1+c_f)} \quad (8)$$

$$c_f = \frac{V_f}{V_m} = \theta_f\ \frac{\rho_d}{\rho_f} \quad (9)$$

where:

$$\theta_f = \frac{(1+w)M_f}{M_m} \quad (10)$$

where ρ_d and ρ_f are respectively the dry density of the matrix and the density of fibers, and w is a water content (considered here as OMC value). M_m and M_f are accordingly the mass of the matrix and the mass of embedded fibers. Obviously, the total number of fibers is N_f deduced as $N_f = N_v\ V_t$, where V_t is a total volume of cover landfill layer. The average value of interfacial shear is given by:

$$\tau_f = \frac{2}{3}\tan(\varphi)\frac{\gamma H}{2} = \frac{1}{3}\tan(\varphi)\,\gamma\, H \quad (11)$$

where φ, γ, and H are respectively the friction angle (=16°, obtained by triaxial tests), the moisture unit weight of the silty sand soil, and the height of the landfill cover layer. The obtained value was around 17 kN/m^3.

On the other side, in the proposed model the soil is bimodular, in the sense that the compressive elastic modulus *Ec* (Figure 4, for cylindrical samples) is different from the tensile elastic modulus E_t (given by (1) and deduced from the experimental results in Figure 6).

2) Application for a Case Study of Landfill Cover and Results Analysis

Figure 10 provides a schema of the finite element mesh of the waste layer and the upper landfill cover. The finite element mesh is denser for a cover layer compared to the waste layer. The δx of each finite element method is fixed at 1 m. Figure 10 also illustrates the boundary conditions, where the symmetric condition is given by ux=0. To generate deflection settlement, the elastic modulus of waste is assumed to increase gradually from x=0 to x=Lw (half of length of the landfill = 45 m). The gradient is $\delta E_w/\ \delta x\ = +0.2$ MPa/m, with the elastic modulus of the waste being E_w = 0.5 MPa at x=0. The values of waste stiffness are only assumed, but unfortunately without any laboratory tests.

By analyzing the rates defined respectively as:

$$r_c = \frac{R_c}{\sigma_c} \text{ and } r_t = \frac{R_t}{\sigma_t} \quad (12)$$

where R_c and R_t are the compressive and tensile strengths measured in the laboratory given by Figures 4 and 6. σ_c and σ_t are respectively the compression stress and tensile stress developed in level η. The tensile fibers in the cover layer can be deduced and the apparent cohesion can be calculated as defined by (4). Naturally, the prediction of deflection, particularly of maximum deflection, is important. It was found that the deflection of cover landfill fiber reinforcement is well reduced, where it decreases with the added embedded fiber content. The vertical displacement calculated in section S1 (maximum deflection, see Figure 10) decreased by around 30% for reinforced soil by fibers (θ_f = 0.5%). Figure 11 depicts the results of the rates r_c and r_t obtained for four sections (S1, S2, S3, and S4).

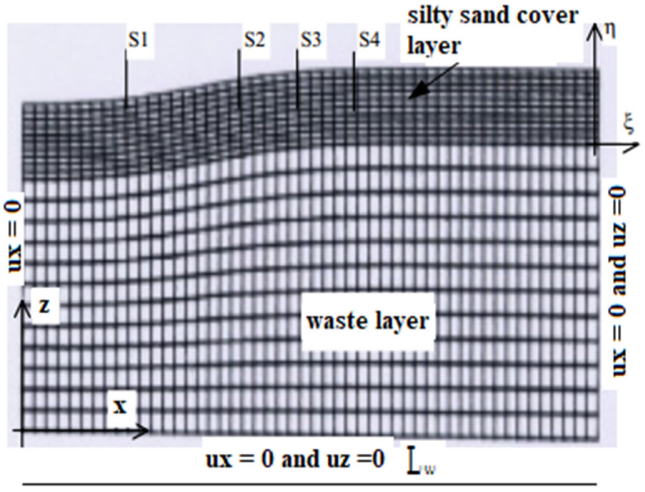

Fig. 10. View of the finite element mesh of the studied landfill and the deflection of the cover layer.

Regarding Figures 12(a)-(d) corresponding to the results of the rates defined for the compression zone and tension zone across the four sections, it can be deduced that in section S1 where the tensile is important (large deformation by tension and tensile stress reaches the tensile strength measured by the four-point bending test in Figure 6). However, in section S4, only compression stress is significant. Globally, the trend of the ratios is similar between S1 and S2 (where the deflection occurred by tension and the tensile stresses were developed), and between S3 and S4 (where the deflection was insignificant, and contraction by compression arose in the same trend of compressive stresses). The contribution of fibers, implicitly included across the apparent cohesion, appears clearly in reducing the tensile stresses more than reducing compressive stresses. This is expected since the short fibers develop only a tensile and eventually flexure resistance and their compressive strength is neglected.

IV. CONCLUSION

The current paper presents a new methodology of the design of the landfill cover layer. The proposed methodology is based on two experimental and numerical approaches. The experimental studies were conducted using unconfined compression and four-point bending tests. From the experimental tests, compressive elastic modulus, tensile elastic modulus, and compressive and tensile strengths were determined. Mohr-Coulomb modulus was implemented considering the bimodular behavior of the tested sandy silt soil in the elasticity framework. The validation of the proposed modeling was conducted based on two different four-point pending tests. The second stage was to implement the model in Code-Bright.

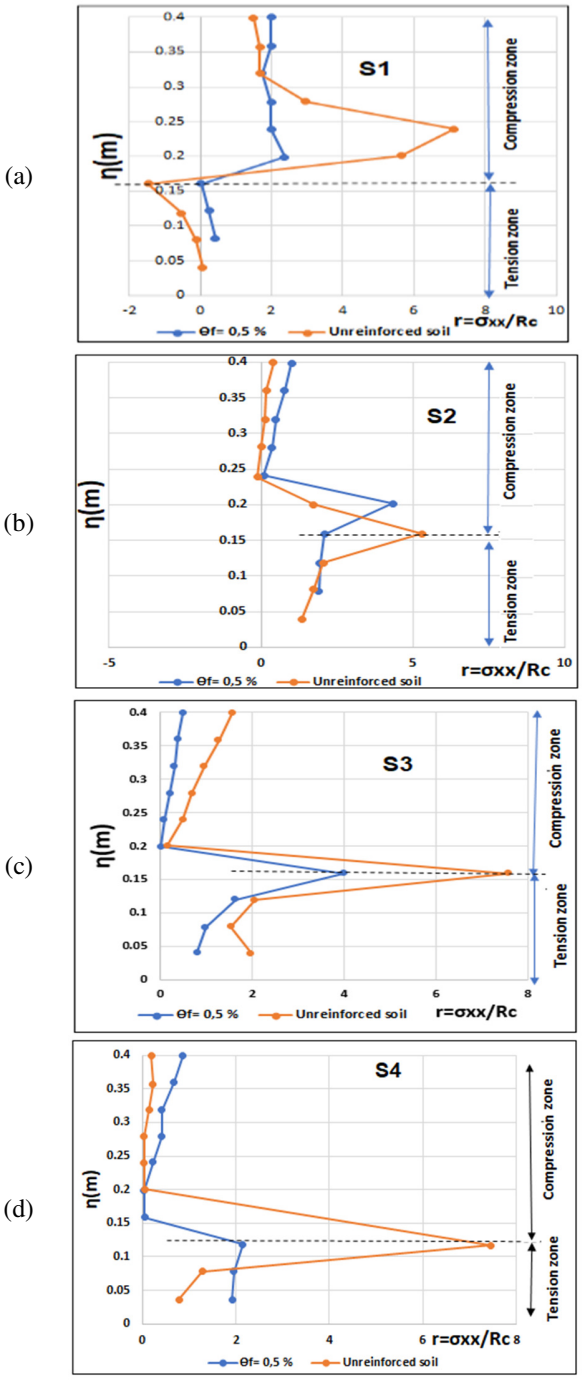

Fig. 11. Experimental and calculated stresses ratios r_c for (a) S1, (b) S2, (c) S3, (d) S4.

The findings of this study pertain that the compacted fine soil employed as a landfill cover can be submitted to high differential deflection and tensile stresses, which may locally exceed the tensile strength and lead to an intensive crack network. This fact compromises the sustainability of the waste landfill. The results demonstrated that the use of the geotextile can minimize deflection, but it is not efficient enough to delay crack initiation and propagation. However, the fiber reinforcement not only increases the tensile strength of the composite and delays the cracks development, but also is an environmental friendly solution. Based on the proposed model, the result analysis suggests that the fibers reduce the tensile stresses in the composite mainly in the deflected and tensile zones.

As mentioned in the introduction, a few studies have focused on the stability of the landfill cover, particularly on the reinforcement role. Thus, this paper briefly discusses the comparison between the contribution of the geotextile on the reinforcement of the soil cover-layer submitted to deflection and the contribution of the short vegetal fibers embedded in the soil. It was revealed that geotextile reduces only the deflection, but it does not play a part in the crack development. However, the fibers contribute to the reduction of crack initiation and development. Consequently, they led to an increase of the tensile strength and tensile stiffness of the composite, which consequently results in the reduction of the deflection deformation. The use of vegetal fibers as a friendly environmental solution is recommended and their positive contribution is well highlighted. This paper conducts a deeply extended research study based on new experimental results and new numerical investigation on the basis of a bimodular constitutive elastoplastic law. Finally, the research about such a complex problem was carried out employing experimental and numerical tools. The former has interesting perspectives concerning the hydromechanical interactions and the investigation of the environmental wetting and drying cycle's role.

ACKNOWLEDGMENT

The authors gratefully acknowledge the approval and the support of this research study by the grant no. ENGA-2022-11-1556 from the Deanship of Scientific Research, Northern Border University, Arar, K.S.A

REFERENCES

[1] B. V. S. Viswanadham, S. Rajesh, and S. S. Sengupta, "Studies on the Integrity of Clay-Rich Soil Liners for Cover Systems of Landfills," in *GeoCongress 2008: Geosustainability and Geohazard Mitigation*, New Orleans, LA, USA, Mar. 2008, pp. 48–55, https://doi.org/10.1061/40970(309)6.

[2] A. Y. Benabdallah and R. Boudour, "Smart Collection of Waste Bread in Algeria Using the Internet of Things," *Engineering, Technology & Applied Science Research*, vol. 12, no. 6, pp. 9483–9486, Dec. 2022, https://doi.org/10.48084/etasr.5280.

[3] M. Naghel, A. Farhi, and A. Redjem, "Household Waste Management Challenges: The Case of M'sila, Algeria," *Engineering, Technology & Applied Science Research*, vol. 12, no. 3, pp. 8675–8682, Jun. 2022, https://doi.org/10.48084/etasr.4925.

[4] "Saudi Arabia - Waste Management," Jan. 03, 2024. https://www.trade.gov/country-commercial-guides/saudi-arabia-waste-management.

[5] A. Saravanan, P. S. Kumar, T. C. Nhung, B. Ramesh, S. Srinivasan, and G. Rangasamy, "A review on biological methodologies in municipal solid waste management and landfilling: Resource and energy recovery," *Chemosphere*, vol. 309, Dec. 2022, Art. no. 136630, https://doi.org/10.1016/j.chemosphere.2022.136630.

[6] S. N. S. Ismail and L. A. Manaf, "The challenge of future landfill: A case study of Malaysia," *Journal of Toxicology and Environmental Health Sciences*, vol. 5, no. 3, pp. 2400–2407, Jun. 2013, https://doi.org/10.5897/JTEHS12.058.

[7] K. Kupusamy *et al.*, "Construction Waste Estimation Analysis in Residential Projects of Malaysia," *Engineering, Technology & Applied Science Research*, vol. 9, no. 5, pp. 4842–4845, Oct. 2019, https://doi.org/10.48084/etasr.2986.

[8] J. Blair and S. Mataraarachchi, "A Review of Landfills, Waste and the Nearly Forgotten Nexus with Climate Change," *Environments*, vol. 8, no. 8, Aug. 2021, Art. no. 73, https://doi.org/10.3390/environments8080073.

[9] B. V. S. Viswanadham, S. Rajesh, P. V. Divya, and J. P. Gourc, "Influence of randomly distributed geofibers on the integrity of clay-based landfill covers: a centrifuge study," *Geosynthetics International*, vol. 18, no. 5, pp. 255–271, Oct. 2011, https://doi.org/10.1680/gein.2011.18.5.255.

[10] M. Amini, H. S. Isfahani, and A. Azhari, "Evaluating water and gas permeability of fiber-modified landfill clay-base liner," *Journal of Environmental Engineering and Science*, vol. 17, no. 3, pp. 120–130, Sep. 2022, https://doi.org/10.1680/jenes.21.00013.

[11] S. Rajesh and B. V. S. Viswanadham, "Hydro-mechanical behavior of geogrid reinforced soil barriers of landfill cover systems," *Geotextiles and Geomembranes*, vol. 29, no. 1, pp. 51–64, Feb. 2011, https://doi.org/10.1016/j.geotexmem.2010.06.010.

[12] H. Trabelsi, M. Jamei, H. Zenzri, and S. Olivella, "Crack patterns in clayey soils: Experiments and modeling," *International Journal for Numerical and Analytical Methods in Geomechanics*, vol. 11, no. 36, pp. 1410–1433, Jul. 2012, https://doi.org/10.1002/nag.1060.

[13] H. Trabelsi, E. Romero, and M. Jamei, "Tensile strength during drying of remoulded and compacted clay: The role of fabric and water retention," *Applied Clay Science*, vol. 162, pp. 57–68, Sep. 2018, https://doi.org/10.1016/j.clay.2018.05.032.

[14] W.-Q. Cheng, Z. Yang, M. Hattab, H. Bian, S. Bouchemella, and J.-M. Fleureau, "Free desiccation shrinkage process in clayey soils," *European Journal of Environmental and Civil Engineering*, vol. 26, no. 13, pp. 6398–6423, Sep. 2022, https://doi.org/10.1080/19648189.2021.1942223.

[15] N. Touze, "Contribution des geosynthetiques au developpement durable," *Revue Francaise de Geotechnique*, no. 160, 2019, Art. no. 1, https://doi.org/10.1051/geotech/2019018.

[16] A. Mittal and A. K. Shrivastava, "Settlement of Landfill Clay Cover Barriers with Geogrid Reinforcement," in *Indian Geotechnical Conference*, Surat, India, 2021, pp. 261–273, https://doi.org/10.1007/978-981-33-6370-0_24.

[17] J. G. Zornberg, "Geosynthetic Reinforcement in Landfill Design: US Perspectives," in *International Perspectives on Soil Reinforcement Applications*, Austin, TX, USA, Oct. 2005, pp. 1–12, https://doi.org/10.1061/40788(167)8.

[18] E. Kravchenko, J. Liu, W. Niu, and S. Zhang, "Performance of clay soil reinforced with fibers subjected to freeze-thaw cycles," *Cold Regions Science and Technology*, vol. 153, pp. 18–24, Sep. 2018, https://doi.org/10.1016/j.coldregions.2018.05.002.

[19] S. Olivella, A. Gens, and J. Carrera, "CodeBright User's Guide," *Barcelona, ETSI Caminos, Canales y Puertos, Universitat Politecnica de Catalunya and Instituto de Ciencias de la Tierra, CSIS*, 1997.

[20] O. Ple, A. Manicacci, J. P. Gourc, and S. Camp, "Flexural behaviour of a clay layer: experimental and numerical study," *Canadian Geotechnical Journal*, vol. 49, no. 4, pp. 485–493, Apr. 2012, https://doi.org/10.1139/t2012-006.

[21] S. Camp, J. P. Gourc, and O. Ple, "Landfill clay barrier subjected to cracking: Multi-scale analysis of bending tests," *Applied Clay Science*, vol. 48, no. 3, pp. 384–392, Apr. 2010, https://doi.org/10.1016/j.clay.2010.01.011.

[22] J.-P. Gourc, O. Ple, P. Villard, and M. Jamei, "Comportement des systemes sols/geosynthetiques en couverture de centres de stockage de dechets," in *African Regional Conference*, Marrakech, Morocco, Dec. 2003, pp. 1–14.

[23] C.-S. Tang, D.-Y. Wang, Y.-J. Cui, B. Shi, and J. Li, "Tensile Strength of Fiber-Reinforced Soil," *Journal of Materials in Civil Engineering*, vol. 28, no. 7, Jul. 2016, Art. no. 04016031, https://doi.org/10.1061/(ASCE)MT.1943-5533.0001546.

[24] M. Zaryoun and M. Hosseini, "Lightweight fiber-reinforced clay as a sustainable material for disaster resilient architecture of future buildings," *Architectural Engineering and Design Management*, vol. 15, no. 6, pp. 430–444, Nov. 2019, https://doi.org/10.1080/17452007.2018.1540968.

[25] X.-Y. Liu, Y. Ye, K. Li, and Y.-Q. Wang, "Stress Path Efforts on Palm Fiber Reinforcement of Clay in Geotechnical Engineering," *Water*, vol. 15, no. 23, Jan. 2023, Art. no. 4053, https://doi.org/10.3390/w15234053.

[26] M. Jamei, P. Villard, and H. Guiras, "Shear Failure Criterion Based on Experimental and Modeling Results for Fiber-Reinforced Clay," *International Journal of Geomechanics*, vol. 13, no. 6, pp. 882–893, Dec. 2013, https://doi.org/10.1061/(ASCE)GM.1943-5622.0000258.

[27] M. Jamei, Y. Alassaf, A. Ahmed, and A. Mabrouk, "Fibers reinforcement of the fissured clayey soil by desiccation," *Magazine of Civil Engineering*, vol. 109, no. 1, 2022, Art. no. 10914, https://doi.org/10.34910/MCE.109.14.